Detection of Incipient Pulp Screen Plugging

Parsa Aryanpour,[a,*] Robert W. Gooding,[a,b] and James A. Olson[a]

Aperture plugging is a phenomenon that limits both the capacity and efficiency of pulp screens, which are critical components of the pulping, recycling, and papermaking processes. An understanding of when and how plugs begin to form can help avoid screen plugging, thus increasing papermaking and recycling efficiency. Small scale, fiber-optic pressure sensors were installed within screen cylinder apertures close to where plugging occurs to understand the mechanism of plug formation. Rotor pressure pulses within the aperture were measured during the plugging event. The pulse shape and magnitude during normal operation showed good agreement with past studies in which traditional pressure transducers were installed on the screen cylinder. However, prior to the onset of aperture plugging, the fiber-optic sensors showed that the variability of the pressure pulses increased and pulse magnitude within the slot decreased. The authors demonstrated that combining these variables by quantifying pulse variability using standard deviation and dividing that by pulse magnitude gave a result that was a strong predictor of aperture plugging.

DOI: 10.15376/biores.20.1.566-587

Keywords: Pulp screening; Aperture plugging; Incipient plugs; Pressure pulses; Plugging indicator

Contact information: a: Department of Mechanical Engineering, The University of British Columbia, 6250 Applied Science Lane, Vancouver, BC, Canada, V6T 1Z4; b: Aikawa Fiber Technologies, 5890 Monkland Avenue, Suite 400, Montreal, QC, Canada, H4A 1G2;
** Corresponding author: parsaary@mail.ubc.ca*

INTRODUCTION

Screening Process

Wood is comprised of cellulose fibers embedded within a lignin matrix. The method used in industry to release the cellulose (pulp) fibers is called “pulping” and can be performed by chemical, thermal, or mechanical means. Recycled furnishes such as paper, cardboard, and other fiber products can also be repulped mechanically to release the constituent pulp fibers. Regardless of the source or pulping method, pulp will contain debris. For virgin pulps, the debris may be bark particles, sand, or shives, which are bundles of fibers that were not separated in the pulping process. For recycled pulps, debris can include plastic fragments, hardened glues, staples, sticky aggregations, glass, and other man-made substances (Smook *et al.* 2016).

Screening is a process by which oversized contaminants are removed from pulp. Pulp screening may also be used to segregate fibers based on their lengths, *i.e.*, fractionation (Olson *et al*. 2000; Olson 2001). In a typical industrial pulp screen, a suspension of pulp fibers in water is fed axially to the annular screening zone between the two main components of the screen, which are the cylinder and rotor. Figure 1 shows a schematic of a generic pulp screen.

During screening, the suspension is bifurcated into 1) an accept stream, flowing radially outward through the cylinder apertures, and 2) a reject stream, flowing axially toward the opposing end of the cylinder. The screen cylinder is open-ended and has apertures in the form of holes or axially-oriented slots. Aperture size is selected to be large enough to provide sufficient capacity (*i.e*. the fiber mass flow rate) but small enough to ensure a high debris removal efficiency. Drilled cylinders (with holes) are robust and are commonly used in the early stages of screening to removal large contaminants. Slotted cylinders have smaller apertures, and are used in the latter stages of screening to remove finer contaminants. Modern slotted cylinders are built as wedge-wire cylinders with contoured wires placed side-by-side and with gaps between to define the slots. The contours on the feed-side cylinder surface are critical to ensure capacity by streamlining the flow through the slots and providing local turbulence to fluidize the fiber suspension.

Fluidization is critical to ensuring fiber flocs are dispersed prior to passing through the slots, which may be only several fiber diameters wide. Increased contour height and decreased wire width increase the turbulence of the flow entering the slots (Halonen *et al.* 1989; Mokamati *et al.* 2010). High-speed videography has been used to observe that on an individual level, the fibers that entered the aperture were pulled in by the vortex created by the contour (Yong *et. al* 2008). Increasing contour size was shown to increase vortex size, which, in turn, increased fiber passage probability.

The rotor is the other performance component of the screen, and there are a range of industrial designs, which can be broadly classified as either “solid core” or “foil type” rotors. A solid-core rotor has drum-like core with hydrodynamic elements attached on its outer surface. This rotor type is more robust and is often used earlier in the earlier stages of stock preparation process or when screening at higher consistency. A foil rotor, on the other hand, has foils with which are positioned close to the cylinder surface by support arms that are connected to a central hub. Foil rotors are used for lower consistency screening applications later in the stock preparation process. While a foil-type rotor was used in this study, the fundamental mechanisms regarding plugging are believed to be generally applicable. Regardless of the design, the rotor spins inside the cylinder to fluidize the pulp suspension, accelerate the flow circumferentially, and create local pressure pulses at the apertures to backflush fibers and oversized particles from the apertures and thus prevent cylinder plugging, which would halt the flow of fibers through the screen and disrupt mill production.

In a mill setting, plugging may be triggered by various factors including: 1) increased accept flow, 2) reduced rotor speed, 3) increased feed consistency, 4) a change in the character in the feed pulp, such as increased fiber length, and 5) reduced reject flow, which may increase reject consistency. Plugging may also result from worn equipment, and the associated reduction in screen contour height or increased cylinder-rotor gap.

Therefore, studying the pressure in the cylinder slots while approaching plugging, and knowing the intensity of forces exerted on the pulp is critical for elucidating screen performance and avoiding plugging. Aperture pressures during a plugging event have not, however, been directly measured in past published works. Past studies have focused on pressure measurements on the inside surface of the cylinder and on the flow through a screen during normal operation, *i.e.*, a screen not approaching plugging (Gooding 1996; Olson 1996; Gonzalez 2002; Feng *et al*. 2003; Delfel 2009; Salem 2013; Li 2020).

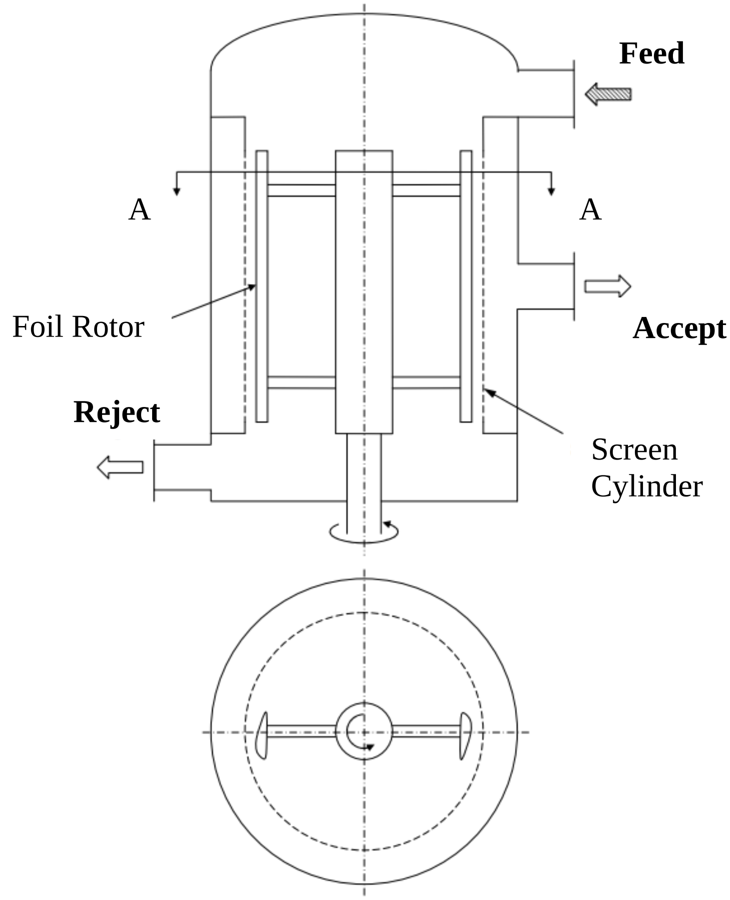

Fig. 1. Schematic of a Laboratory Pulp Screen (Delfel 2009)

Pulp Fibers and Rheology

Fibers are much larger in length than they are in width (*i.e.*, large aspect ratio), and this plays an important role in the associated pulp rheology. Crowding factor (N) is a dimensionless parameter that helps to characterize fiber-fiber contact and the degree of flocculation in water suspensions (Kerekes and Schell 1992). Its value can be calculated using Eq. 1,

$$N \approx \frac{5C_m L_w^2}{\omega} \tag{1}$$

where C_m is the mass-based pulp consistency (%), L_w is the length-weighted average fiber length (m), and ω is fiber coarseness (kg/m) defined as the weight per unit length of fiber. Certain values of N have been associated with regimes where critical behavior changes occur in pulp suspensions (Mason 1950; Soszynski and Kerekes 1988; Kerekes and Schell 1992; Martinez *et al*. 2001; Celzard *et al*. 2009). Notably, $N \approx 60$, known as the "rigidity threshold" (Celzard *et al*. 2009) is the point at which each fiber contacts on average about three other fibers. This is an important value because fibers are restrained by three-point contact and without shear they bend elastically and become inter-locked due to the mechanical strength added to the network by the normal forces creating friction at each contact point (Derakhshandeh *et al*. 2011). An absence of turbulence or decaying turbulence, such as is found in the wakes of pumps and mixers, are favorable conditions for floc formation and subsequently an increase in fiber suspension heterogeneity in mass and strength (Kerekes 1983; Derakhshandeh *et al*. 2011). Other forces, such as those from hooking of curved fibers or from chemical flocculants, may add mechanical strength to the fiber network (Kerekes *et al*. 1985; Hubbe 2007).

Rotor Pressure Pulses

Several studies (Gooding 1996; Gonzalez 2002; Feng *et al*. 2003) analyzed pressures generated by foil rotors in detail. Some general observations are that pulse magnitude decreases with increasing pulp consistency, and that the magnitude of the suction portion of the pressure pulse increases with V_t^2 in high-speed foil rotation regimes, *i.e.*, where flow is turbulent. However, power demands during screening also must be considered, as they increase proportionally to V_t^3 (Olson *et al*. 2004).

Delfel (2009) performed pulsation tests using a 60-mm AFT EP foil with a 0° angle-of-attack and 5-mm rotor-cylinder gap. He used a small industrial screen with a 203-mm (8 in) nominal diameter wedge-wire cylinder with 0.9-mm contour height, 3.2-mm wire width, and 0.15-mm slot width. A similar screen was used in the current study, with the cylinder contour height and wire width being 1.2 and 2.6 mm, respectively. For pressure measurements, Delfel (2009) used a 3.8-mm diameter sensor installed flush with the feed side of the cylinder wires, spanning a portion of a wire and two slots. Similar results to previous feed-side cylinder wall pressure measurements were found, and Delfel (2009) derived a non-dimensional pressure coefficient to normalize pressure by V_t^2. He identified $V_t \gtrsim 12$ m/s and $V_s \lesssim 1$ m/s as the parameters that created uniform pulse shapes with the highest degree of backflushing (*i.e.*, -0.35 C_p negative pulse strength) with the explanation that too slow a V_t and too high a V_s creates a non-turbulent boundary layer around the foil and therefore flow separation. A faster foil has a more turbulent boundary layer that is more resistant to flow separation and stalling - a phenomenon that is also encouraged when increasing V_s and removing material from around the foil.

Plugging Fundamentals

Fluid-driven plugging, as is the case in pulp screening, has been less studied than plugging in gravity-driven flows. Though they share similarities, fluid-driven models require additional insight into factors such as particle concentrations, fluid velocities, fluid-particle interactions, and other hydrodynamic effects (Guariguata *et al*. 2012). Villalba *et al*. (2023) performed a plugging study using rigid nylon rods that were intended to simulate pulp fibers. They used particle tracking velocimetry to observe plugging for a sudden contraction (flow aligned with the aperture) and a T-junction (flow normal to the aperture) and categorized plugging into the three sequential steps of nucleation, accumulation, and permanent blockage or blockage followed by release.

Nucleation was found to be caused *via* two mechanisms: single-particle bridging across the aperture or localized mechanical entanglement of the particles, *i.e.*, flocculation. The former was caused when fiber length was equal or greater than aperture width, while the latter was caused by a combination of aggregation and arch-formation at all fiber-length to aperture-width ratios, and more dominantly at higher concentrations. Single-fiber bridging typically resulted in plug densification during the subsequent accumulation phase (*i.e.*, enlargement of the obstruction area with time) and led to permanent plugging. Flocculation typically did not create permanent plugs but displayed a behavior consisting of intermittent plugging and releasing that occurred when the flocs grew to the point of reducing flow area but then broke apart, likely due to the hydrodynamic forces overpowering the friction forces between the aperture and the fibers. Flocculation was more common directly after entry into the aperture space, though it also happened to a lesser extent in the area upstream of the aperture (Villalba *et al*. 2023).

Salem (2013) investigated the effects of pulp type, V_t and V_s on pulp screen capacity and plugging using an MR8 pulp screen equipped with NACA 0015 foils of 40 mm chord and 6° angle-of-attack, and a cylinder with a contour height of 0.9 mm, wire width of 3.2 mm, and slot width of 0.15 mm. He plotted the V_t needed to induce screen failure at various V_s, feed consistencies, and blends of softwood and hardwood fibers. He found nearly parallel lines of increasing V_t for increasing V_s for each consistency. After extrapolating the lines for each consistency and finding the intercepts on the V_t axis, a directly proportional relationship was established between consistency and plugging V_t. The nearly-zero intercept suggested, as expected, that for a 0% fiber concentration (*i.e.* water), a V_t of 0 m/s would be sufficient to prevent screen plugging.

A "compressed plug friction" model was proposed for aperture plugging in pulp screens (Martinez *et al*. 1999). According to this model, a pulp plug was compressed while passing into a slotted aperture. Plugging occurred when the frictional forces on the slot walls exceeded the net pressure from the rotor-induced pulse and the pressure differential across the cylinder. Its validity was supported by industrial tests with a range of different slot geometries and slot velocities.

Objective and Overall Approach

Gaining insight into incipient aperture plugging and developing an early indicator of plugging were the objectives of this study. The approach taken was to bring a pilot pulp screen to the point of plugging by either increasing the average speed of pulp through the cylinder slots (V_s) or decreasing the rotor tip speed (V_t). Slot pressure sensor data were then studied to a) compare the shape, magnitude, and variability of the pressure pulses in the slots created by the rotor foils with similar studies based on sensors mounted on the cylinder wall (Gooding 1996; Gonzalez 2002; Feng *et al*. 2003; Delfel 2009) and b) attempt to detect incipient plugging based on the characteristics of the pressure signal in the slot. This has not been possible using traditional pressure and flow measurements and allowed for the exploration of the hypothesis that incipient aperture plugging is brought on by an increasing accumulation of fiber flocs at the slot throat, which would create pressure changes that can be detected by the novel slot pressure sensors.

EXPERIMENTAL

MR8 Pulp Screen and Flow Loop

A Beloit MR8 pilot-scale pulp screen (Fig. 2) at the UBC Pulp and Paper Centre was used to conduct the experiments. This model of screen has a cylinder measuring 203 mm (8 in) in diameter and 254 mm in length. The cylinder selected for the study was an unchromed AFT MacroFlow™ wedge-wire cylinder with a 0.15-mm slot width, 3.2-mm wire width, and 1.2-mm contour height. A variable frequency drive (VFD) controls the speed of the AFT EP™ Rotor inside the cylinder which, for the MR8 screen, has two foils (60-mm chord length). For this test, the foils were set at a 0° angle-of-attack with a 2.6-mm gap to the cylinder.

For a particular trial, either water or a pulp suspension was pumped from a tank of 300-L capacity to the screen by a VFD-equipped open-impeller pump, and then returned through the accept and reject lines to the tank so that the screen loop operated in continuous recirculation. Ball valves installed on the accept and reject lines were modulated remotely using LabView™ control software. Magnetic flow meters and flush-diaphragm pressure transmitters monitored the flow rates and pressures on the feed, accept, and reject lines. Flow and pressure data and the rotational speed of the rotor were collected at 1000 Hz and saved using LabView.

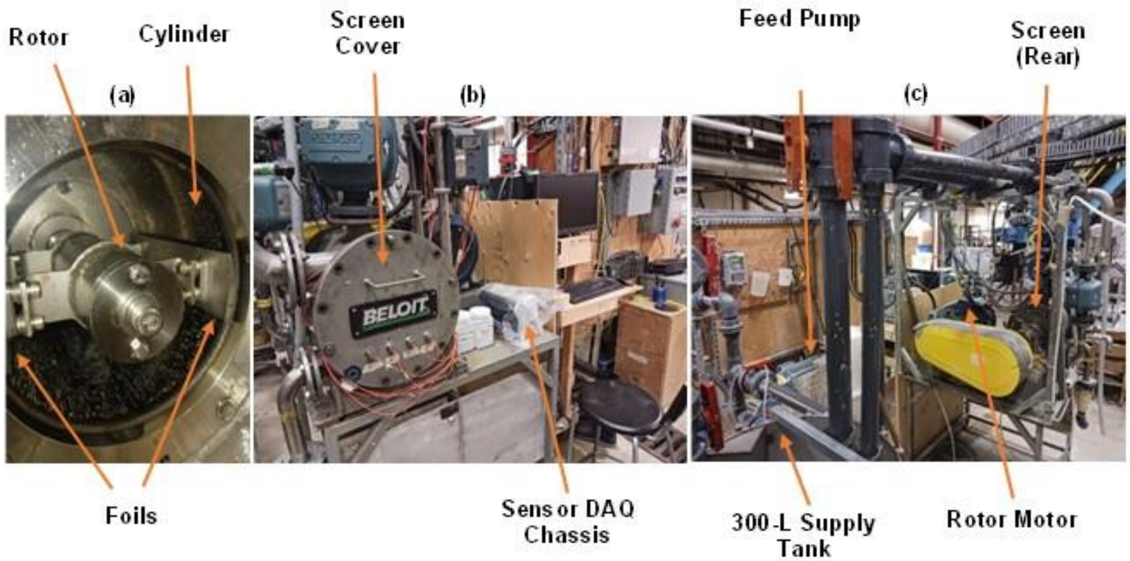

Fig. 2. (a) Two rotor foils inside the MR8 pulp screen (with the left foil only partly visible); (b) Slot sensor (orange) wires extend out of Beloit screen cover; (c) MR8 pilot plant testing apparatus

Pulp

Two market pulps with very different fiber length and coarseness distributions were used: a northern bleached softwood kraft (NBSK) produced from a spruce, pine, and fir furnish from the interior of British Columbia, and a bleached hardwood kraft (BHK) pulp produced from an aspen furnish in Alberta. An OpTest Fiber Quality Analyzer™ was used to measure the length-weighted average fiber length (L_w), coarseness, and average fiber diameter of the two pulps (Table 1), giving results similar to literature values (Reeves *et al*. 1994; Gharehkhani *et al*. 2015; de Assis *et al*. 2019).

The pulp suspension for a given trial was prepared by reslushing dry pulp sheets in the supply tank, which was typically filled to a volume of approximately 250 L with water at ~15 °C. The tank was equipped with a VFD-controlled mixer that was used to reslush the pulp, without the pump in operation, until no flakes were apparent in a collected sample. The returning flows to the tank provided substantial agitation, but to be certain that there would be no stratification or flocculation, the mixer was run continuously during all trials. A new pulp suspension was prepared for each trial to minimize the influence of any change in pulp characteristics during recirculation for the approximately 0.5 h of operation of a typical trial.

Table 1. Physical Properties of Pulp Fibers

Pulp Type	L_w (mm)	Coarseness (kg/m)	Diameter (µm)
Softwood	2.50	13.4×10^{-8}	28.6
Hardwood	0.78	10.3×10^{-8}	21.9

In-Slot Pressure Measurement

To gain novel insight into the plugging event in the cylinder slots, a 0.2-mm diameter hole was machined in the side surface of a screen cylinder wire (Wire B in Fig. 3) at the slot "throat", *i.e.*, the point of minimum distance between adjacent wires. The hole served as a pressure tap that connected to a 0.64-mm hole that received a fiber-optic pressure sensor (FISO^{TM} FOP-MIV). To support the sensor, aligned guide-holes were machined in the four adjacent wedge wires (Wires C to F in Fig. 3). The pressure tap was assumed to fill with water during the start of a trial in a way that would transmit pressures to the sensor without detectable delay. Likewise, the pressure tap and fiber-optic cable were assumed to not cause any build-up of fibers that would disturb the flow or interfere with the passage of fibres, as was supported by a visual inspection of the slots after each test.

Due to sensor fragility and the need to thoroughly pressure wash the cylinder after each trial, fasteners could not be used, and the guide-holes machined into the wires were form-fitting, *i.e.*, with essentially the same 0.64-mm diameter as the polyimide-sheathed sensor portion close to the measurement tip (Fig. 5). The guide-hole narrows in Wire B and connects with the 0.2-mm pressure tap to create a "shoulder" section, preventing the sensor from protruding out of Wire B and entering the slot, potentially disturbing the flow, or bending or becoming damaged by the slot flow or direct impact with fiber flocs and debris. A second slot pressure location was made 180° from the first to provide a redundant measurement. Sensors were not interchanged between the two measurement locations. The sensors were placed in the mid-axial position of the cylinder, where the rotor is assumed to have accelerated the suspension to the terminal rotational velocity, and where the influence of flow disturbances near the entrance and exit of the screening zone is minimalized (Yu 1994; Atkins 2007; Delfel 2009). The axial midpoint is also intended to represent the median degree of pulp thickening that will occur along the length of the cylinder (Gonzalez 2002).

The 8-cm polyimide tip section of the fiber-optic sensor (Fig. 5) was secured using Kapton polyimide tape after exiting the guide-holes (Fig. 4a). A portion of the PVC-sheathed section of the sensor (Fig. 5) was then attached to the mid-axial support ring of the cylinder (Fig. 4b), where it would have minimal interference with the exiting accept flow through the screen slots. The sensor wires were then passed axially along the cylinder, through the top flange and then through the cover of the pulp screen itself where the wires were connected to the FISO FPI-HS-1 signal conditioning module (Fig. 4c) that sampled the sensor readings at 2500 Hz. A FISO EVO-SD-5 chassis provided power for the sensors and signal conditioners and connected to a computer *via* USB.

After installation in the slots, the sensors were zeroed in atmospheric pressure before each trial to measure gauge pressure, which is the same as the MR8 pressure transducers. Recordings of the slot pressure sensors were then started on the FISO Evolution DAQ software (version 2.2.0.0) at the same time as the start of MR8 sensor recordings on LabView. Because there was no link between the two groups of sensors, a lag time of approximately 1 to 2 s was assumed between the start of the two groups of recordings. Additionally, the two slot sensors were not precisely synchronous, and the length of the recordings for the two sensors typically varied by a few thousandths of a second.

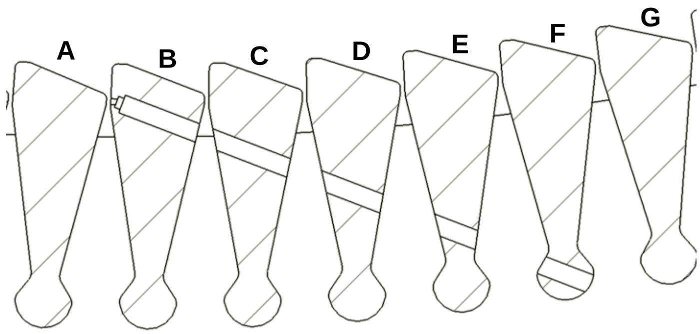

Fig. 3. Wire assembly as modified to accept the fiber-optic pressure sensor

(a) (b) (c)

Fig. 4. (a) Polyimide-sheathed portion of a sensor (Fig. 5) entering Wire F (Fig. 3); (b) PVC sheathing of sensor secured on a ring using Kapton polyimide tape with silicone adhesive; (c) SCAI connectors of the sensors inserted in the signal conditioner

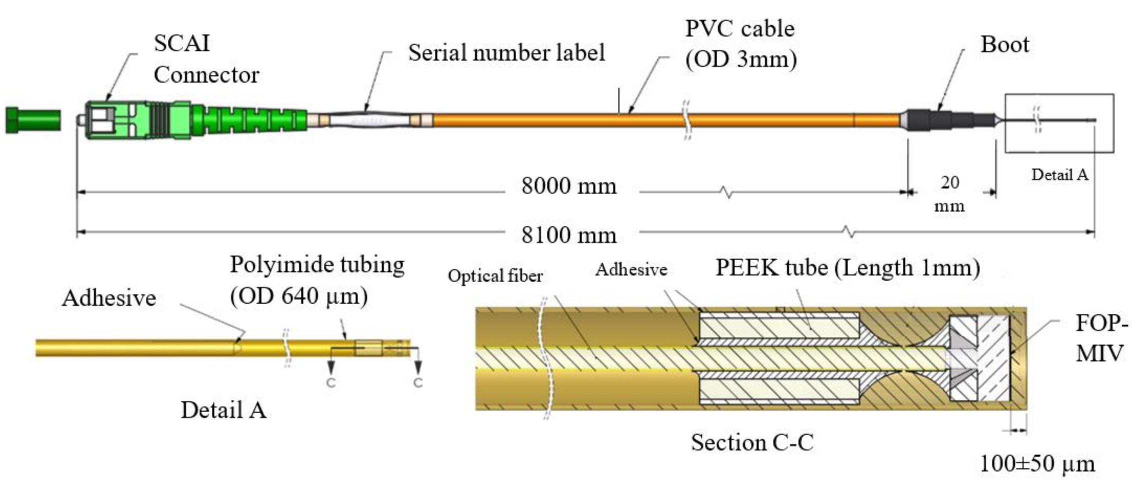

Fig. 5. FOP-MIV fiber-optic sensor details (FISO 2023)

Trial Protocol

General

In any trial, the pulp or water would be prepared as discussed previously. The screen rotor would be started at the specified initial V_t. The pump would be started with the accept valve closed and the reject valve fully open. The accept valve would be gradually opened until the target initial V_s was reached, and then the reject valve was gradually closed until the volumetric reject ratio (*i.e.*, the reject flow divided by the feed flow) reached a value of 17%, which is a typical industrial value. At this point, the sample and debris valves would be opened and closed momentarily to allow trapped air to escape, which would otherwise skew sensor readings. A fixed value for the feed pump VFD was set, producing approximately 125 kPa of feed pressure (with the exact value depending on the pulp consistency), which supports a suitable range of V_s (~0.7 m/s to 2.4 m/s) at the target volumetric reject ratio. Moreover, the increased feed and reject line pressures that occur post-plugging would still stay below the safety limit of approximately 250 kPa.

Plugging trial protocol

Plugging was triggered using two alternate approaches: decreasing V_t or increasing V_s. For the first method, performed on the full range of consistencies, V_s was kept at a constant value of 1.5 m/s while decreasing V_t from 23 m/s down to the point of plugging by increments of 1 rpm (~ 0.01 m/s). For the second method, performed with 1.5% feed consistency, three different V_t values were chosen based on the results of the V_t study: one below and two above the plugging V_t. V_t was kept constant, while V_s was increased from 0.7 m/s to the point of plugging by opening the accept valve in 1% increments while adjusting the reject valve to maintain a constant R_v.

The tests were concluded when plugging occurred. Data logging was terminated, and the pump, rotor, and tank mixer were then stopped. The tank was emptied, and the cylinder was removed from the screen housing. The slot pressure sensors were then carefully extracted from the cylinder. Prior to starting the next trial, the cylinder was pressure-washed, and the fiber-optic sensor tips were inspected and then gently shaken in lukewarm water for 1 min to clear any fibers from the tip surfaces.

Pressure Pulses

As discussed, pressure pulses have been previously measured on the feed-side surface of the screen cylinder, but the current study provided first-ever measurements of the pulses within the slot throat. Similarly to Delfel (2009), to analyze the pulse form without the presence of small variations generated by turbulence, ensemble averages of 100 consecutive pulses were calculated. To account for possible manufacturing and tolerancing differences in the fiber-optic sensors, sensor housings, cylinder wires, and rotor-cylinder gaps, pressure data were assessed independently for each of the two sensor locations. There was no discernable difference between the pulses produced by one foil or the other, so they were not separated. Pressures detected at the different sensor locations on the screen cylinder were very similar, but the pulses were not combined due to the lack of precise synchronization between the slot sensors, as mentioned earlier.

To compare pressure pulses, it is important to isolate the pressure changes caused exclusively by the rotor and exclude other factors, such as changes to the screen line pressures, to achieve different V_s and R_v. The pressure measured at the slots was thus zeroed by a freestream pressure value that is as unaffected as possible by the action of the rotor. Previous studies (Gonzalez 2002; Feng 2003; Atkins 2007; Luukonen *et al*. 2007; Delfel 2009) have chosen this freestream value to be the mean pressure over a set timeframe or the mean pressure between pulses. However, mean pressure (sampled instantaneously every 10 s while decreasing V_t by ~1 rpm/s or ~0.01 m/s^2) was found to be influenced by the rotor disturbances, *i.e.*, a higher V_t creates a larger magnitude of the suction portion of the pressure pulse, leading to a decrease in the mean value. Median pressure was found to be less affected by V_t and was thus chosen as the freestream value. As a result, the median pressure specific to each of the 100 constituent pulses of the ensemble average was subtracted from each pulse. As reported previously (Delfel 2009), the constituent pulses to determine the average were aligned using their minimum values to prevent any loss in pulse magnitude due to factors such as small V_t fluctuations. Once the average was obtained, it was also necessary to normalize the elapsed time for each pulse to compare pulses of different V_t.

RESULTS AND DISCUSSION

Effect of V_t and V_s on the Pressure Pulse Variability

Water-based trials

Pulse-to-pulse variability is shown in Fig. 6 with an example of 100 water-based pulses and the resultant average pulse. The average pulse is represented by markers featured every few data points, a practice that is repeated in other figures across this work to distinguish different lines in a plot. To compare pulses of different V_t (Fig. 7) once the average was obtained, it was necessary to normalize the elapsed time for each pulse (Aryanpour 2024). Figure 7 shows this average pulse along with 99% confidence intervals (CI) using the normal distribution. This figure shows good overall agreement with previous pressure measurements made on the feed-side cylinder surface (Gonzalez 2002; Feng 2003; Delfel 2009), which suggests that for normal screen operation, the pressure pulse signature on the cylinder surface is representative of that in the slot.

The current work expands on using CI in that CI reflects the standard deviation, and standard deviation was used to quantify pulse variability, which was found to be a relevant element for gauging screen runnability and incipient plugging. One may assume a baseline level of variability as the foil rotates in water, which is in part due to turbulence levels but also due to flow separation from around the foil as V_t decreases or V_s increases. Once pulp is added, pulse variability will further be influenced by fiber accumulations in the slot, as shown below. The increased variability is intrinsic to the transient fiber accumulations that characterize incipient plugging. However, the addition of pulp also increases fluid viscosity and thus decreases baseline fluid turbulence, meaning that while water benchmarks are good references, they cannot be used as absolute bases for comparison.

A dashboard was built to monitor both the traditional pulp screen sensor readings, primarily feed, accept and reject line pressures, accept and reject flow rates, rotor speed, and the novel slot pressures used in this study. The dashboard helped visualize that just prior to cylinder plugging, the variability of the ensemble-average constituent pulses increased. The standard deviation compared to the ensemble-average was then calculated at each acquisition point encompassing a pulse and averaged for each pulse, as shown below. The peak-to-peak pulse magnitude (P_M, *i.e.*, $P_{max} - P_{min}$) was used to normalize the deviation.

As an example, when measuring a 20 Hz foil passage frequency (1200 rpm, corresponding to V_t = 12.4 m/s) with the slot sensors acquiring data at 2500 Hz, a pulse would span 125 acquisition points (k = 125). There were 100 pulses (i = 100) used to create an ensemble average. For each of the 125 acquisition points that span an average pulse, there were 100 data points that were used to arrive at a final averaged value. The standard deviations of those ensemble-average pressure pulses were calculated for a 20 Hz pulse following Eq. 2:

$$P_D = \frac{\sum_{k=1}^{125} \sqrt{\frac{\sum_{i=1}^{100}(P_{i\ at\ pt.k} - P_{avg\ at\ pt.k})^2}{100-1}}}{125} \tag{2}$$

Values of P_D can then be normalized by P_M to create normalized deviation (P_D'). This contextualizes P_D because, for instance, a value of P_D = 10 Pa could signify very little or very considerable deviation levels depending on whether the P_M is 30 Pa or 300 Pa. Beyond the issue of normalization, a parameter that combines the influence of pulse variability with the influence of pulse diminution is especially valuable in assessing incipient failure given that both effects may be present.

As shown in Figs. 8 and 9, the magnitude of P_D increased with increasing V_t, but it was relatively independent of V_s. Figures 10 and 11 demonstrate that P_M decreased with decreasing V_t until ~ 5 m/s ($Re \approx 2.5 \times 10^5$), at which point the flow was most likely fully laminar and the foil movement created very little pulsation. It should be noted that the industrial range of operation for V_t is generally from 10 to 20 m/s – and so the behavior below 10 m/s is of limited practical interest. Figures 10 and 11 also show that V_s has only a small influence on P_M at any value of V_t.

Combining the above results to illustrate P_D' (Fig. 12) shows that for the industrial range of operation, P_D' was relatively low (*i.e.*, less than 0.3) and uniform. The high values of P_D' at low V_t and especially below 5 m/s may be because the very weak pulse became progressively indistinguishable from the background variability.

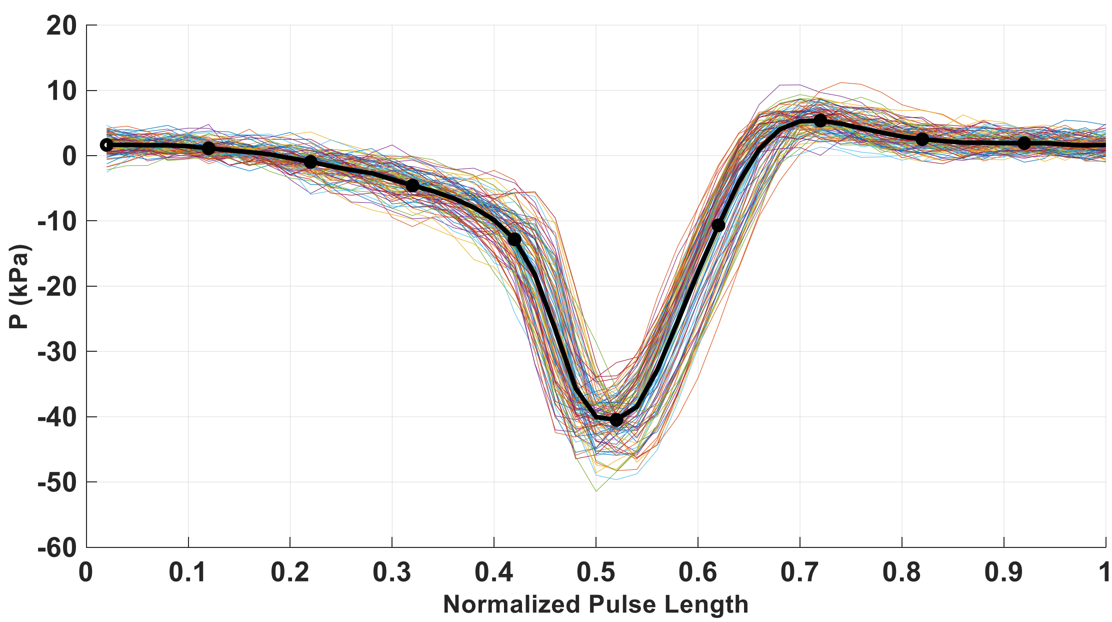

Fig. 6. Ensemble of 100 pressure pulses at V_t = 15.1 m/s and V_s = 1.6 m/s, creating an average pulse (black line with markers)

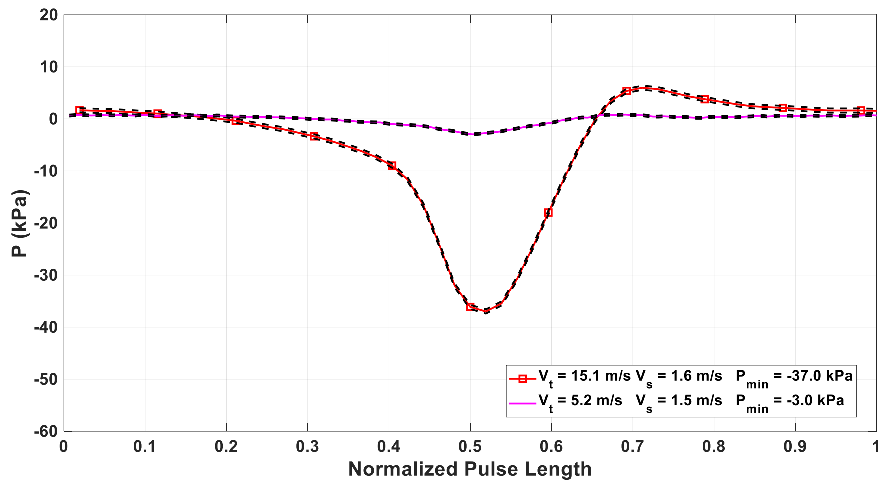

Fig. 7. Pressure pulse examples with 99% confidence intervals shown in black

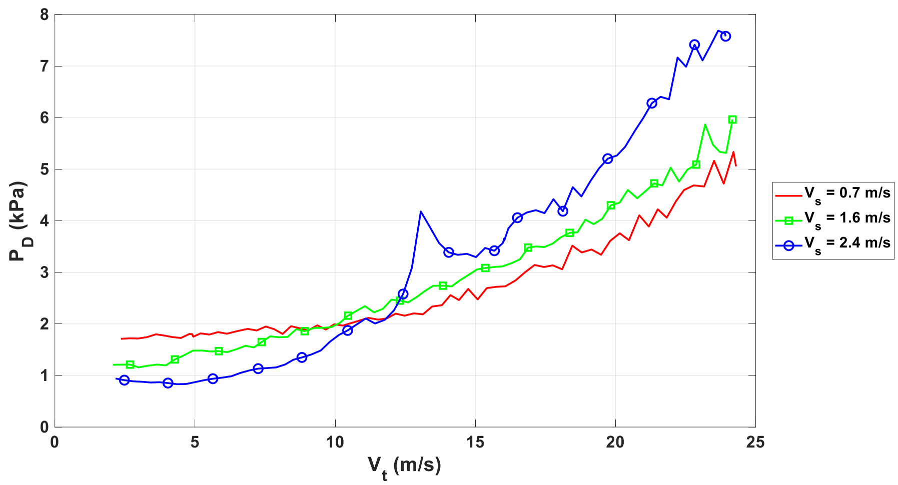

Fig. 8. Deviation of pressure pulses *versus* V_t for water

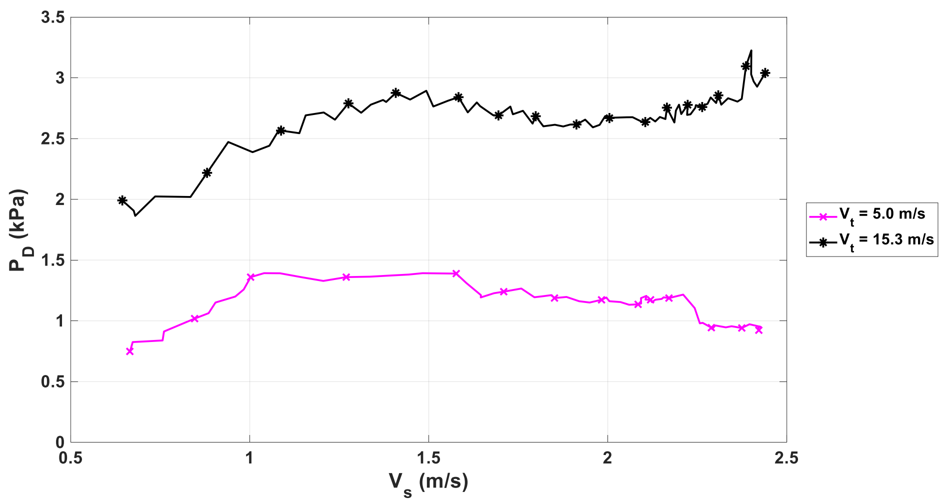

Fig. 9. Deviation of pressure pulses *versus* V_s for water

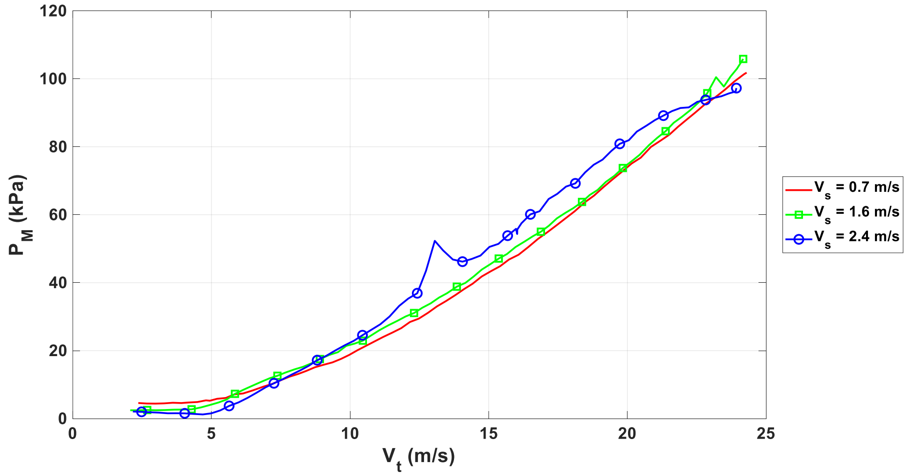

Fig. 10. Amplitude of pressure pulses *versus* V_t for water

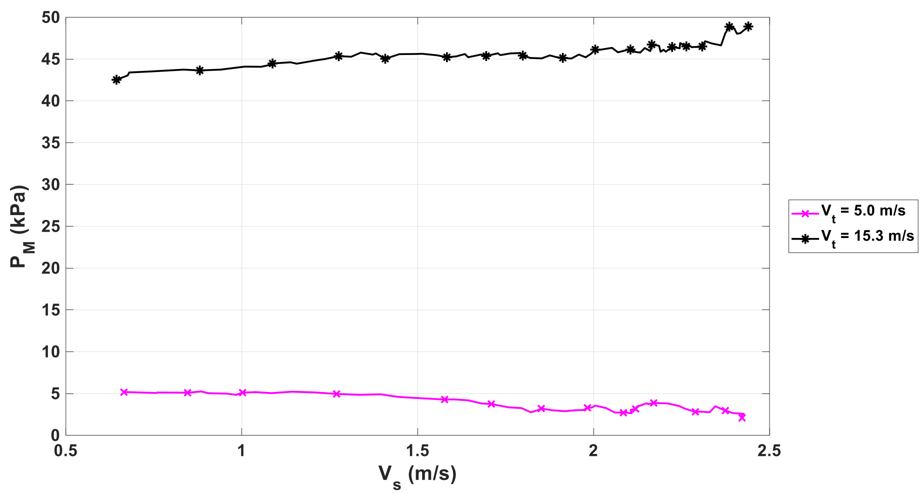

Fig. 11. Amplitude of pressure pulses *versus* V_s for water

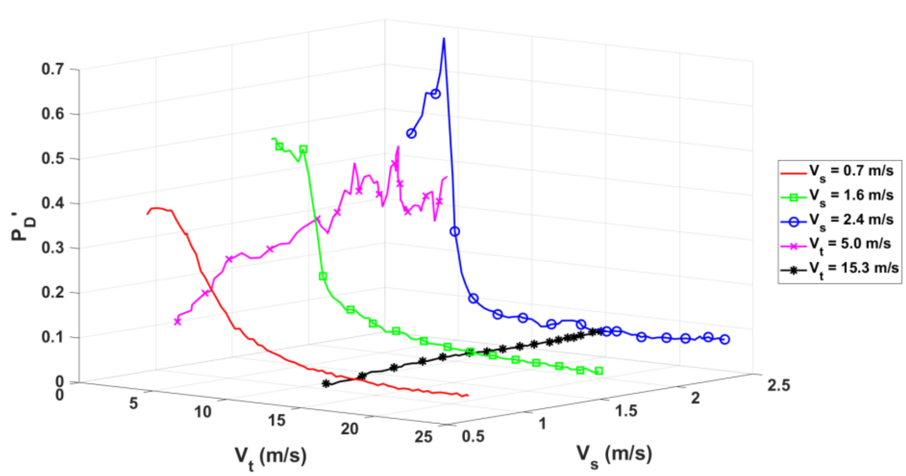

Fig. 12. Pulse deviation normalized by amplitude *versus* V_t and V_s for water

Pulp-based trials

As with the water trials shown above, *P*D decreased with decreasing V_t with pulp (Fig. 14). Close to plugging (~1 to 2 m/s V_t above plug trigger value of V_{tp}), however, there was a period where *P*D increased ~0.5 kPa for most cases. This is likely indicative of incipient plugging affecting the flow. Flocs that are increasingly large and stagnant for longer time periods within the slot could be causing disturbances and fluctuations in the pressure pulses. Incipient plugging effects have been studied by Villalba *et al*. (2024a), who applied image analysis to quantify and analyze the intermittent plug-and-release slot plugging event that had been established and documented by Hoffmann *et al.* (2024), albeit for round screen apertures that were many times larger than the modern small-slotted apertures. The results shown in Fig. 14 provide support for a plug-and-release mechanism under representative conditions for a modern screen configuration. Villalba *et al*. (2024b) applied a similar analysis to identify fluctuations in screen feed and accept line pressures near plugging.

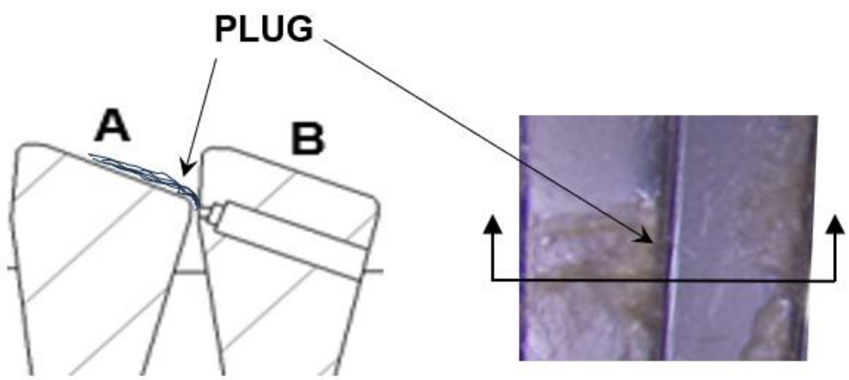

(a) (b)

Fig. 13. (a) Fibers are drawn to represent a plug slightly above the slot pressure measurement port (shown previously in Fig. 3) in the throat of the slot between wires “A” and “B”; b) a top-view of a plugged slot in an industrial screen, with fibers extending from the slot between the two wires shown in (a). The drawing in (a) represents a sectional view of (b)

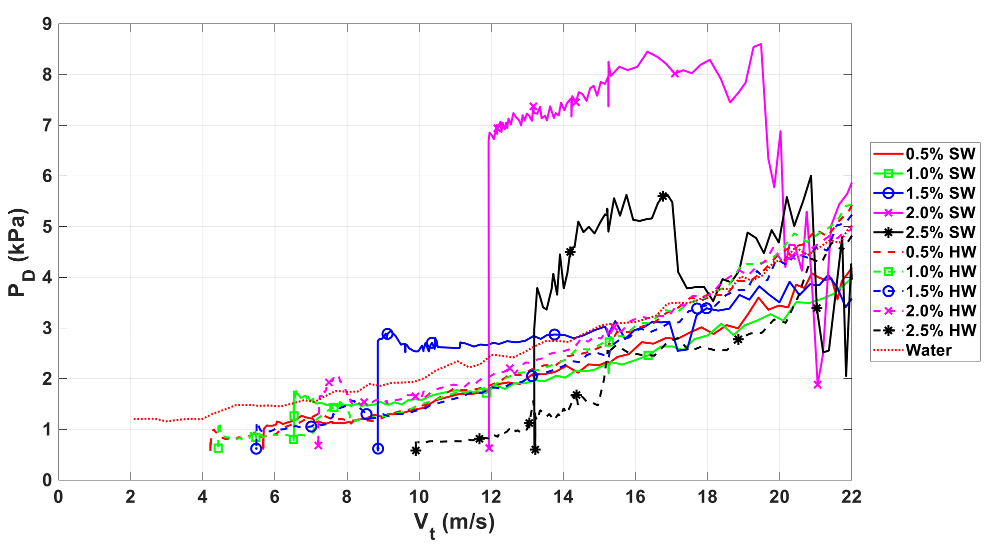

Fig. 14. Pressure pulse deviation for V_t plugging trigger (V_s ~ 1.5 m/s)

The main exceptions in Fig. 14 are the 2.0% and 2.5% SW suspensions that demonstrate much higher P_D than the others and do not follow a trend similar to water, indicating that at the higher SW concentrations, the fluid rheology and plugging dynamics are distinctly different. In general, and for all of the curves in Fig. 14, it is reasonable that at lower V_t the rotor is less effective in breaking down and dispersing fiber flocs. This would lead to having flocs becoming immobilized and dewatered within the screen slot and fewer individual fibers passing through the screen cylinder.

An indication of incipient plugging is also seen in the plot of P_M *versus* V_t (Fig. 15). P_M levels are generally similar to the water benchmark, but as V_t approaches the critical value at which plugging happens, P_M decreases abruptly compared to the water benchmark. This suggests that as the screen enters the plug-and-release behavior of incipient plugging, not only does P_D increase, but as one would expect, P_M (as measured in the slot) decreases.

The diminution of the pulse amplitude can also be demonstrated by normalizing the pressure pulses for the 1.5% SW example across various V_t (Fig. 16) and representing the pulses in pressure coefficient form similar to past works (Gooding 1996; Gonzalez 2002; Feng *et al*. 2003; Pinon *et al*. 2003; Delfel 2009). Doing so allows for visualization of pulse diminution as a result of effects other than decreasing V_t, *i.e.*, as a result of incipient plugging. The pulse form is essentially unchanged above 10 m/s as V_t decreases from 12.95 m/s to 10.93 m/s. However, a further decrease of ~1 m/s, to 9.81 m/s, resulted in an almost 30% decrease in the minimum value of C_p ($C_{p,min}$). Finally, an additional decrease of ~1 m/s to 8.85 m/s led to plugging and the elimination of the pressure pulse as sensed within the slot. After plugging, the slot pressure is very close to the accept line pressure. The disappearance of the pulse at plugging leads to the finding that the plugs are at least partially formed above the slot pressure measurement position, as shown in Fig. 13 and therefore almost fully dampen the foil-induced pulsations.

P_D' can then be plotted (Fig. 17), which encompasses both the increase in P_D and decrease in P_M caused by the incipient plugging phenomenon. This leads to a more systematic measure of screen runnability and plugging prediction using the slot sensors. All suspensions started at the same value of ~0.05 P_D' at 22 m/s V_t, specifically a V_t that was sufficiently above the plugging values for the pulps and screening configuration considered here, whereby it can be assumed that the cylinder slots were clear of plugs. Decreasing the V_t led to an increase in P_D' and, other than the 2.0% and 2.5% SW suspensions which displayed a linear behavior, showed a clear exponential trend that can be used to assess incipient plugging. The point at which plugging happened was also a common value of ~0.3 across all tests, which helped to locate any of the individual tests in terms of how close the screen was to failure. The water benchmark followed the same trend up to the point of ~5 m/s. The point at which an individual trial deviated from the water benchmark can be taken as the beginning of incipient plugging and in an industrial setting this parameter might be used in real time to assess screen runnability or choose the point at which the minimum V_t could be set while allowing for a "design factor" that respects the variability of the feed pulp consistency and character in an industrial setting. It is preferable to not run the rotor faster than needed because a small gain in screening runnability (*e.g.*, going from P_D' ~0.1 to ~0.05) would be exchanged for a considerable increase in energy consumption, which has been shown to increase with the cube of V_t (Olson *et al*. 2004; Dylke *et al*. 2008).

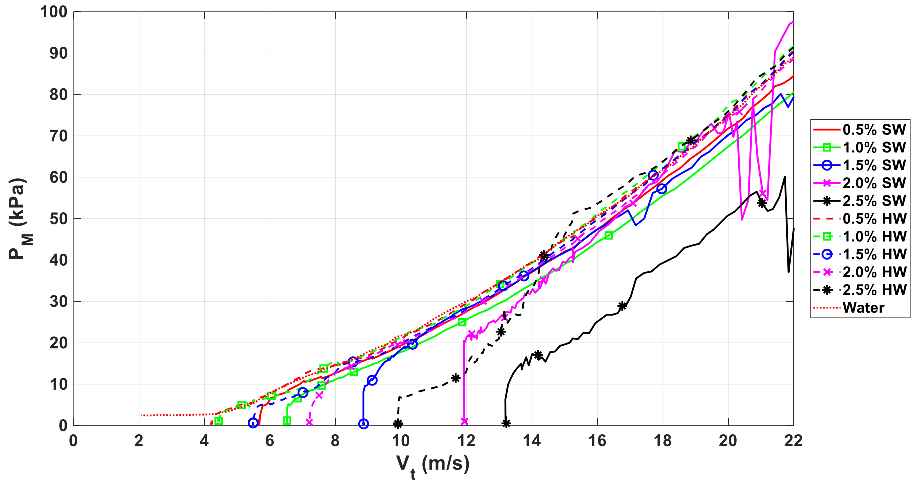

Fig. 15. Pressure pulse amplitude for V_t plugging trigger (V_s ~ 1.5 m/s)

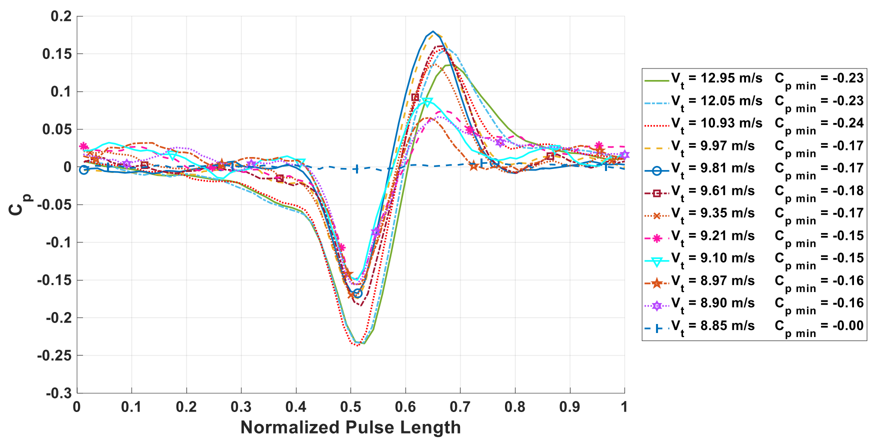

Fig. 16. Pressure pulse coefficients at V_t far from plugging (> 10 m/s), close to plugging (< 10 m/s), and at plugging (8.85 m/s) for a V_t plugging trigger with 1.5% SW (V_s ~ 1.5 m/s). Each pulse is plotted based on an ensemble average of 100 pressure pulses

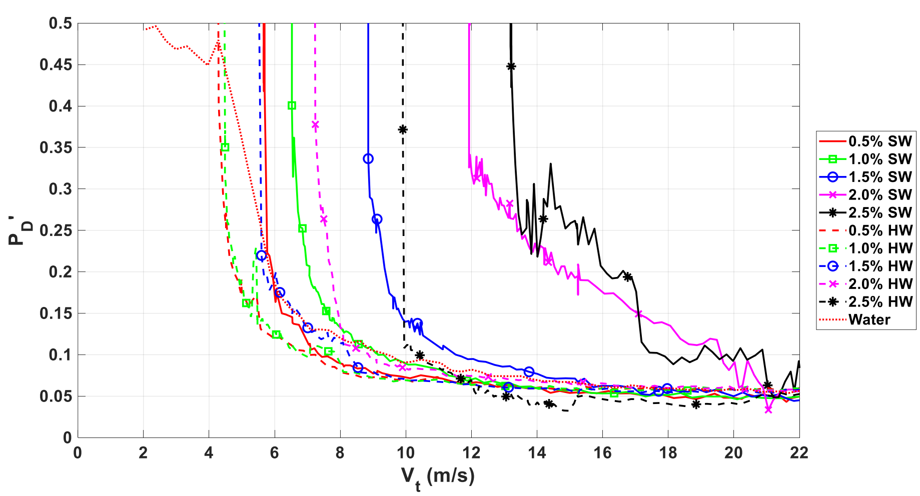

Fig. 17. Normalized pressure pulse deviation for V_t plugging trigger (V_s ~ 1.5 m/s)

The same exercise can be performed for V_s plug triggering (Figs. 18 and 19). There are some differences compared to V_t , which must be considered when using P_D' as a means to evaluate screen runnability.

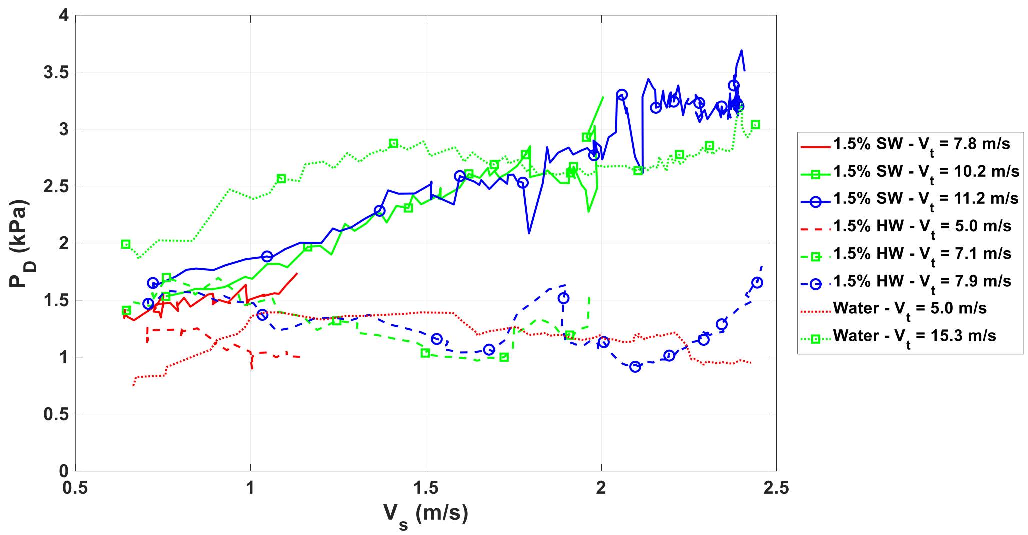

Fig. 18. Pressure pulse deviation for V_s plugging trigger

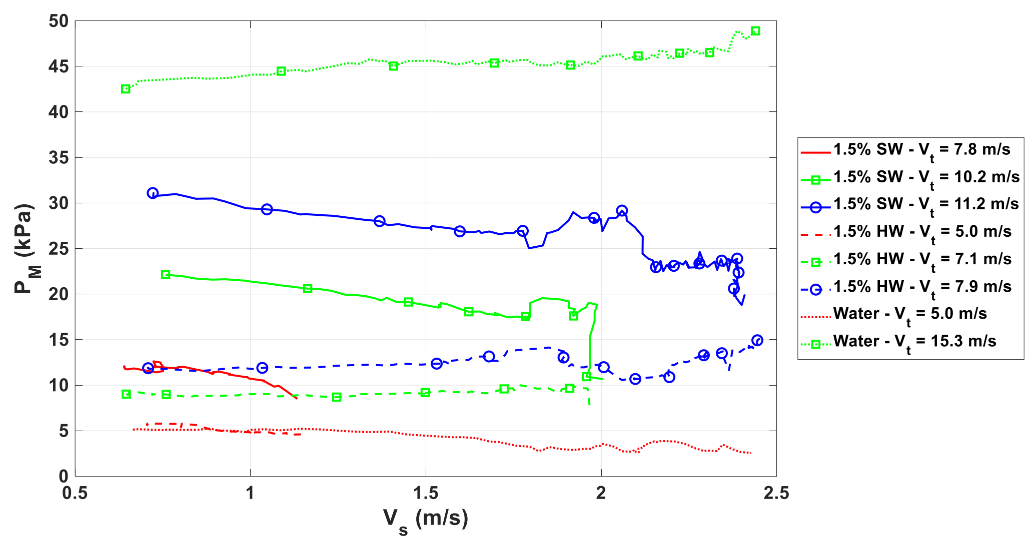

Fig. 19. Pressure pulse amplitude for V_s plugging trigger

Inputs in V_s triggering tests showed less resolution than for V_t triggering (by a factor of ~20 or more), which means that near plugging, there may be a more sudden period of plugging, reflected in more sudden, jagged P_D' increases. V_t triggering can be done more incrementally because decreasing V_t by the smallest step of 1.0 rpm translates to ~0.01 m/s. For a typical trial starting at V_t of 22 m/s and decreasing to ~5 to 10 m/s, ~1200 to 1700 individual steps in V_t would span the trial. However, for V_s triggers, to avoid reject thickening at a volumetric reject ratio of ~17%, the lowest V_s was set at 0.7 m/s for all trials.

Thus, even at the highest V_s failure point of 2.4 m/s, an entire trial would span only around 60 steps in opening the accept valve by 1% increments (~40% open to ~100% open).

The process of V_s triggering may also be physically different to V_t triggering: Higher V_s causes an increase in the flow of fiber into the slot, while the frequency and strength of the backflushing action is relatively unaffected. For V_t plugging, however, there is a decrease in backflushing strength and frequency while the fiber flow into the slot is unaffected. Both lead to persistent fiber accumulations, which lead to plugging, but they approach this point from different directions, which could be a source of different incipient plugging properties.

Despite the above differences, P_D' can still be used quite effectively for evaluating screen runnability when performing V_s triggering. Because these experiments were designed to be performed with the same feed pulp consistency of 1.5%, the way to create a range of experiments was to vary the point of V_s failure by changing V_t for each experiment. This means that a single water test cannot be used as a benchmark for the range of V_s triggering tests. As opposed to a 2D representation for V_t triggering tests (Fig. 17), which share the same V_s, a 3D representation (Fig. 20) is more appropriate to visualize P_D' results of V_s triggering tests. In Fig. 20, the five black lines representing benchmarks of water P_D' (shown previously in Fig. 12) were used to construct a 3D surface. In all but one trial (1.5% HW, V_s = 1.1 m/s at failure) a large increase in P_D' was seen, above the water benchmark surface, before plugging occurred. For example, one can imagine a surface that is 0.05 P_D' above the water benchmark surface and notice that typically, ~0.3 to 0.5 m/s before reaching the plugging V_s (*i.e.*, V_{sp}), P_D' crossed the 0.05 P_D' threshold above the water benchmark. Another consideration for the V_s triggering trials is to focus on the two trials with V_t > 10 m/s, which represent values within the industrially relevant range of speeds. Because the two trials were set at close V_t values, one can, as demonstrated in Fig. 21, pinpoint a common critical P_D' value of ~0.15, at which point both trials were close to creating plugs ~0.5 m/s V_s before reaching plugging.

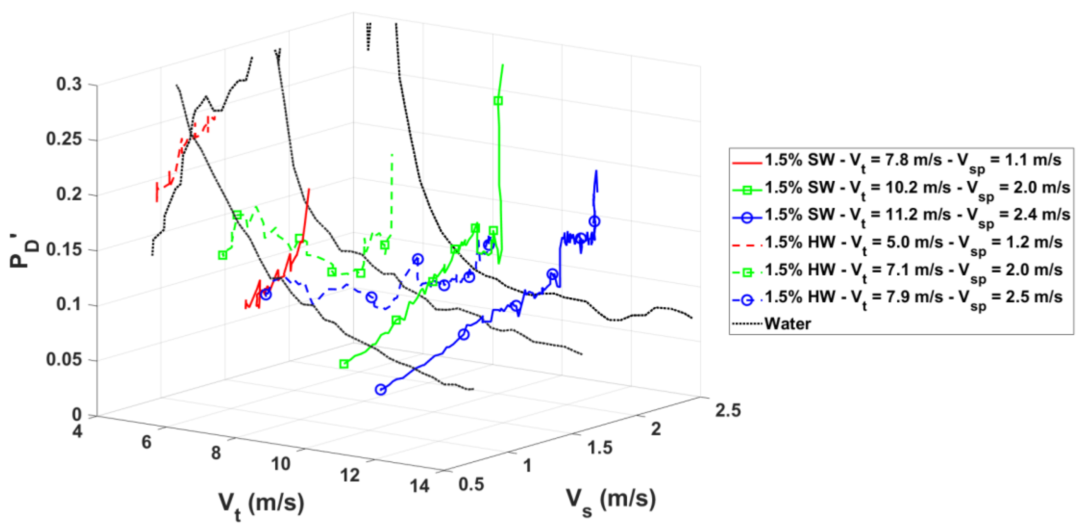

Fig. 20. Normalized pressure pulse deviation for V_s plugging trigger (V_{sp} denotes the V_s at which plugging happened)

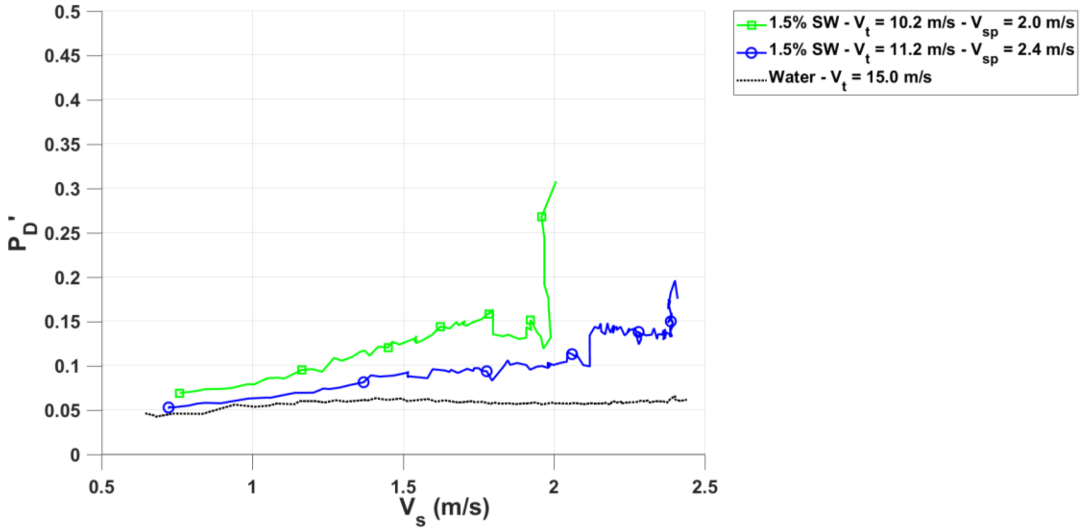

Fig. 21. Normalized pressure pulse deviation for V_s plugging trigger of pulp trials with $V_t > 10$ m/s (V_{sp} denotes the V_s at which plugging happened)

CONCLUSIONS

A small fiber-optic pressure sensor was installed into a pressure screen to measure the pressure pulses created by the rotor directly in the slot aperture. Pressure pulse data was collected during aperture plugging for a wide range of operating conditions. From this data, it was concluded that:

1. During normal operation, the pressure pulses measured in the slot are similar in form and strength to those captured with traditional cylinder wall measurements, albeit with minor differences that are likely due to the passing flow and more suppressed measurement location.
2. As the cylinder approaches plugging, the slot pressure sensors provide an indication of incipient plugging, from both a) increased pulse variability and b) reduced pulse amplitude, which supports the plug-and-release model of incipient plugging under conditions representative of the current industrial practice.
3. The normalized standard deviation of an ensemble of pressure pulses P_D', measured within the slot, provides a quantifiable measure of incipient plugging. A critical P_D' value of approximately 0.3 was suggested for a broad range of pulp types and feed consistencies when plugging was induced by reduced V_t. A lower critical P_D' value of approximately 0.15 was suggested for plugging induced by increased V_s. Further study is required to determine the critical P_D' for a wider range of plugging scenarios.

ACKNOWLEDGMENTS

The financial and technical contributions of Natural Sciences and Engineering Research Council (NSERC), Aikawa Fiber Technologies, UBC Pulp and Paper Centre

(PPC), UBC BioProducts Institute (BPI), Canfor Pulp Products, and Mercer International are gratefully acknowledged.

REFERENCES CITED

Aryanpour, P. (2024). *Plugging of Pulp Screen Apertures*, MASc Thesis, The University of British Columbia, Vancouver, BC, Canada. DOI: 10.14288/1.0441527

Atkins, M. J. (2007). *Axial Variations and Entry Effects in a Pressure Screen*, Ph.D. Thesis, The University of Waikato, Hamilton, New Zealand.

Celzard, A., Fierro, V., and Kerekes, R. (2009). "Flocculation of cellulose fibres: New comparison of crowding factor with percolation and effective-medium theories," *Cellulose (London)* 16(6), 983-987. DOI: 10.1007/s10570-009-9314-0

de Assis, T., Pawlak, J., Pal, L., Jameel, H., Venditti, R., Reisinger, L. W., Kavalew, D., and Gonzalez, R. W. (2019). "Comparison of wood and non-wood market pulps for tissue paper application," *BioResources* 14(3), 6781-6810. DOI: 10.15376/biores.14.3.6781-6810

Delfel, S. (2009). *A Numerical and Experimental Investigation into Pressure Screen Foil Rotor Hydrodynamics*, Ph.D. Thesis, The University of British Columbia, Vancouver, BC, Canada. DOI: 10.14288/1.0067925

Derakhshandeh, B., Kerekes, R. J., Hatzikiriakos, S. G., and Bennington, C. P. J. (2011). "Rheology of pulp fibre suspensions: A critical review," *Chemical Engineering Science* 66(15), 3460-3470. DOI: 10.1016/j.ces.2011.04.017

Dylke, E., Fowler, L., Pflueger, C., and Olson, J. A. (2008). "Advanced pulp screen rotor technology provides electrical energy savings at Canfor-Northwood," *Pulp and Paper Canada* 109(2), 39-43.

Feng, M., Olson, J. A., Ollivier-Gooch, C. F., Xia, J., and Gooding, R. W. (2003). "A computational fluid dynamic (CFD) tool for advanced pulp screen foil rotor design," in: *ABTCP Conference*, Sao Paulo, Brazil.

Feng, M. M. (2003). *Numerical Simulation of the Pressure Pulses Produced by a Pressure Screen Foil Rotor*, Master's Thesis, The University of British Columbia, Vancouver, BC, Canada. DOI: 10.14288/1.0080954

FISO. (2023). "Medical pressure monitoring," FISO, (https://fiso.com/wp-content/uploads/2018/10/MC-00263_-Medical-Pressure-Monitoring-Product-Datasheet_R7.pdf), Accessed 15 Oct 2023

Gharehkhani, S., Sadeghinezhad, E., Kazi, S. N., Yarmand, H., Badarudin, A., Safaei, M. R., and Zubir, M. N. M. (2015). "Basic effects of pulp refining on fiber properties—A review," *Carbohydrate Polymers* 115, 785-803. DOI: 10.1016/j.carbpol.2014.08.047

Gonzalez, J. A. (2002). *Characterization of Design Parameters for a Free Foil Rotor in a Pressure Screen*, Master's Thesis, The University of British Columbia, Vancouver, BC, Canada. DOI: 10.14288/1.0081003

Gooding, R. W. (1996). *Flow Resistance of Screen Plate Apertures*, Ph.D. Thesis, The University of British Columbia, BC, Canada. DOI: 10.14288/1.0058507

Guariguata, A., Pascall, M. A., Gilmer, M. W., Sum, A. K., Sloan, E. D., Koh, C. A., and Wu, D. T. (2012). "Jamming of particles in a two-dimensional fluid-driven flow," *Physical Review E: Covering Statistical, Nonlinear, and Soft Matter Physics* 86(6), article 061311. DOI: 10.1103/PhysRevE.86.061311

Halonen, L., Ljokkoi, R., and Peltonen, K. (1989). "Improved screening concepts," in:*Tappi Pulping Conference*, Seattle, WA, USA, pp. 61-66.

Heise, O. (1992). "Screening foreign material and stickies," *Tappi Journal* 75(2), 78-81.

Hoffmann, J. D., Craig, D. C., and Gooding, R. (2024). "Pulp screening: In-screen imaging and analysis," *ResearchGate* (In-press).

Hubbe, M. A. (2007). "Flocculation and redispersion of cellulosic fiber suspensions: A review of effects of hydrodynamic shear and polyelectrolytes," *BioResources* 2(2), 296-331. DOI: 10.15376/BIORES.2.2.296-331

Kerekes, R., and Schell, C. J. (1992). "Characterization of fibre flocculation regimes by a crowding factor," *Journal of Pulp and Paper Science* 18, 32-38.

Kerekes, R. J. (1983). "Pulp flocculation in decaying turbulence: A literature review," *Journal of Pulp and Paper Science* 9(3), 86-91.

Kerekes, R. J., Soszyński, R. M., and Tam Doo, P. A. (1985). "The flocculation of pulp fibres," in: *Papermaking Raw Materials, Trans. of the VIII^th^ Fund. Res. Symp. Oxford*, Manchester, England, pp. 265-310. DOI: 10.15376/frc.1985.1.265

Li, W. (2020). *Numerical Study of a Transient Bifurcating-Flow Near Slotted Apertures*, Master's Thesis, The University of British Columbia, Vancouver, BC, Canada. DOI: 10.14288/1.0387345

Luukonen, A., Delfel, S., Olson, J. A., Pflueger, P., and Ollivier-Gooch, C. (2007). "Numerical simulations of pressure pulses produced by a solid core pressure screen rotor," in: *61st Appita Annual Conference and Exhibition*, Gold Coast, Australia, pp. 265-271.

Martinez, D., Buckley, K., Jivan, S., Lindstrom, A., Thiruvengadaswamy, R., Olson, J., Ruth, T., and Kerekes, R. (2001). "Characterizing the mobility of papermaking fibres during sedimentation," *The Science of Papermaking*, Trans. of the XIIth Fund. Res. Symp. Oxford, Manchester, England, pp. 225-254. DOI: 10.15376/frc.2001.1.225

Martinez, D. M., Gooding, R. W., and Roberts, N. (1999). "A force balance model of pulp screen capacity," *Tappi Journal* 82(4), 181-187.

Mason, S. G. (1950). "The motion of fibres in flowing fluids," *Pulp and Paper Canada* 51(5), 93-100.

Mokamati, S., Olson, J. A., and Gooding, R. W. (2010). "Numerical study of separated cross-flow near a two-dimensional rough wall with narrow apertures and suction," *Canadian Journal of Chemical Engineering* 88(1), 33-47. DOI: 10.1002/cjce.20243

Olson, J. (2001). "Fibre length fractionation caused by pulp screening, slotted screen plates," *Journal of Pulp and Paper Science* 27(8), 255-261.

Olson, J., Allison, B., and Roberts, N. (2000). "Fibre length fractionation caused by pulp screening. Smooth-hole screen plates," *Journal of Pulp and Paper Science* 26(1), 12-16.

Olson, J. A. (1996). *The Effect of Fibre Length on Passage Through Narrow Apertures*, Ph.D. Thesis, The University of British Columbia, Vancouver, BC, Canada. DOI: 10.14288/1.0058501

Olson, J. A., Turcotte, S., and Gooding, R. (2004). "Determination of power requirements for solid core pulp screen rotors," *Nordic Pulp & Paper Journal* 19(2), 213-217. DOI: 10.3183/npprj-2004-19-02-p213-217

Pinon, V., Gooding, R. W., and Olson, J. A. (2003). "Measurements of pressure pulses from a solid core screen rotor," *Tappi Journal* 2, 9-12.

Reeves, R. H., Plantikow, J. D., Smith, L., Oriaran, T. P., Awofeso, A. O., and Worry, G. L. (1994). "Soft high strength tissue using long-low coarseness hesperaloe fibers," US Patent No. 5320710.
Salem, H. J. (2013). *Modeling the Maximum Capacity of a Pulp Pressure Screen*, Ph.D. Thesis, The University of British Columbia, Vancouver, BC, Canada. DOI: 10.14288/1.0103345
Smook, G. A., Knovel, A. G. E., and Project, A. (2016). *Handbook for Pulp & Paper Technologists*, (Fourth Ed.), *Tappi Press*, Peachtree Corners, GA.
Soszynski, R. M., and Kerekes, R. J. (1988). "Elastic interlocking of nylon fibers suspended in liquid: Part 1. Nature of cohesion among fibers," *Nordic Pulp & Paper Research Journal* 3(4), 172-179. DOI: 10.3183/npprj-1988-03-04-p172-179
Villalba, M. E., Daneshi, M., and Martinez, D. M. (2023). "Characterizing jamming of dilute and semi-dilute fiber suspensions in a sudden contraction and a T-junction," *Physics of Fluids* 35(12), article ID 123339. DOI: 10.1063/5.0178933
Villalba, M. E., Olson, J. A., and Martinez, D. M. (2024a). "Understanding the limits of a screening operation. Part 1: Characterization of screen plugging," *BioResources* 19(2), 2404-2416. DOI: 10.15376/biores.19.2.2404-2416
Villalba, M. E., Olson, J. A., and Martinez, D. M. (2024b). "Understanding the limits of screening operation. Part 2: Characterizing the operational window," *BioResources* 19(2), 2990-3000. DOI: 10.15376/biores.19.2.2990-3000
Yong, A., Mokamati, S., Ouellet, D., Gooding, R. W., and Olson, J. A. (2008). "Experimental measurement of fibre motion at the feed surface of a pulp screen," *Appita : Technology, Innovation, Manufacturing, Environment* 61(6), 485-489. DOI: doi/10.3316/informit.410422178927402
Yu, C. J. (1994). "Pulsation measurement in a screen. Part I: Pulse signature and magnitude of S-shape rotor," in: *Tappi Engineering Conference*, San Francisco, CA, USA, pp. 767-782.

Article submitted: August 22, 2024; Peer review completed: October 5, 2024; Revised version received and accepted: October 23, 2024; Published: November 19, 2024.
DOI: 10.15376/biores.20.1.566-587